ADVANCED HEALTHCARE MATERIALS
www.advhealthmat.de

Protein-Engineered Biomaterials to Generate Human Skeletal Muscle Mimics

*Debanti Sengupta, Penney M. Gilbert, Kyle J. Johnson, Helen M. Blau, and Sarah C. Heilshorn**

Skeletal muscle function, which is essential in the human body, can be lost due to injury, trauma, or diseases such as muscular dystrophy, prompting the need for *in vitro* models of human skeletal muscle tissue. *In vitro* tissue models are indispensable in performing quantitative studies of injury and disease progression as well as in providing sources of tissue for potential regenerative medicine therapies. An ideal bioengineered model of skeletal muscle should promote myoblast (muscle cell precursor) alignment as well as subsequent myoblast fusion into mature, multinucleated muscle cells known as myotubes. Accordingly, we report the development of an engineered protein biomaterial that promotes the alignment and fusion of primary human myoblasts into organized and differentiated myotubes. Furthermore, these aligned human myotubes exhibit markers of functional maturation including organization of sarcomeres (the force-generating apparatus within muscle) and induced contractility upon electrical stimulation.

D. Sengupta
Stanford University
Department of Chemistry
466 Lomita Mall, Moore Building,
Room 271, Stanford, CA 94305-4045, USA
Dr. P. M. Gilbert
Stanford University
School of Medicine
Department of Microbiology and Immunology
Baxter Laboratory for Stem Cell Biology
269 Campus Drive, Clinical Sciences Research Center,
Room 3200, Stanford, CA 94305-5175, USA
K. J. Johnson
Stanford University
Department of Materials Science and Engineering
466 Lomita Mall, Moore Building,
Room 271, Stanford, CA 94305-4045, USA
Prof. H. M. Blau
Stanford University
School of Medicine
Department of Microbiology and Immunology
Baxter Laboratory for Stem Cell Biology
269 Campus Drive, Clinical Sciences Research Center,
Room 4215, Stanford, CA 94305-5175, USA
Prof. S. C. Heilshorn
Stanford University
Department of Materials Science and Engineering
476 Lomita Mall, McCullough Building,
Room 246, Stanford, CA 94305-4045, USA
E-mail: heilshorn@stanford.edu

DOI: 10.1002/adhm.201200195

To achieve this goal, we utilize a protein-engineered biomaterial to investigate the roles of biomaterial surface topography and cell-adhesion ligand density in promoting human muscle cell fusion *ex vivo*. These two material properties are selected due to previous reports that they influence the morphology and differentiation of murine myogenic cells, including primary mouse myoblasts and the transformed C2C12 cell line.[1–8] Mouse-derived cells are used in the vast majority of *in vitro* muscle studies and have contributed greatly to our knowledge of muscle cell biology. However, few studies to date have used human muscle biopsies to isolate primary myoblasts,[9–14] which are the most clinically relevant cell type, and a systematic analysis of biomaterial design criteria is lacking for human myoblasts. Here, we characterize the interactions of human primary myoblasts with a family of engineered biomaterials, and, for comparison, include the standard mouse-derived C2C12 cell line. While our results clearly demonstrate that human myoblasts, similar to C2C12 cells, are sensitive to surface topography and cell-adhesion ligand density, we also identify behavioral discrepancies indicating that C2C12 cells do not faithfully recapitulate the human myoblast response to biomaterial cues.

Our protein-engineered biomaterial enables precise manipulation of several scaffold properties, thus combining the cytocompatibility of naturally-derived materials with the tunability of synthetically-designed materials.[15,16] These protein biomaterials are compatible with soft lithography microfabrication techniques, allowing production of reproducible topographical surface features on cell-relevant length scales (Figure S1 of the Supporting Information (SI)). In addition, the concentration of cell-adhesion ligands within these biomaterials can be exactly specified without altering the surface topography or the mechanical properties.[15,17] Fibronectin is an essential component of the basement membrane of muscle fibers *in vivo*.[18] Therefore, a fibronectin-derived amino acid sequence that includes the cell-adhesive RGD peptide is directly incorporated into the engineered protein backbone (Figure S1 of the SI). Four repeats of this fibronectin sequence are interspersed with an elastin-like sequence that confers mechanical resilience to the scaffold, as required for contractile muscle tissue mimics.

Using this protein-engineered construct, we designed a family of biomaterials with repetitive topographical grooves ranging in spacing from 20–200 μm and RGD ligand densities of 96500, 482500, and 965000 ligands/μm^2. Primary myoblasts isolated from human biopsies as well as C2C12 cell-line cultures remain adherent and viable on all biomaterials

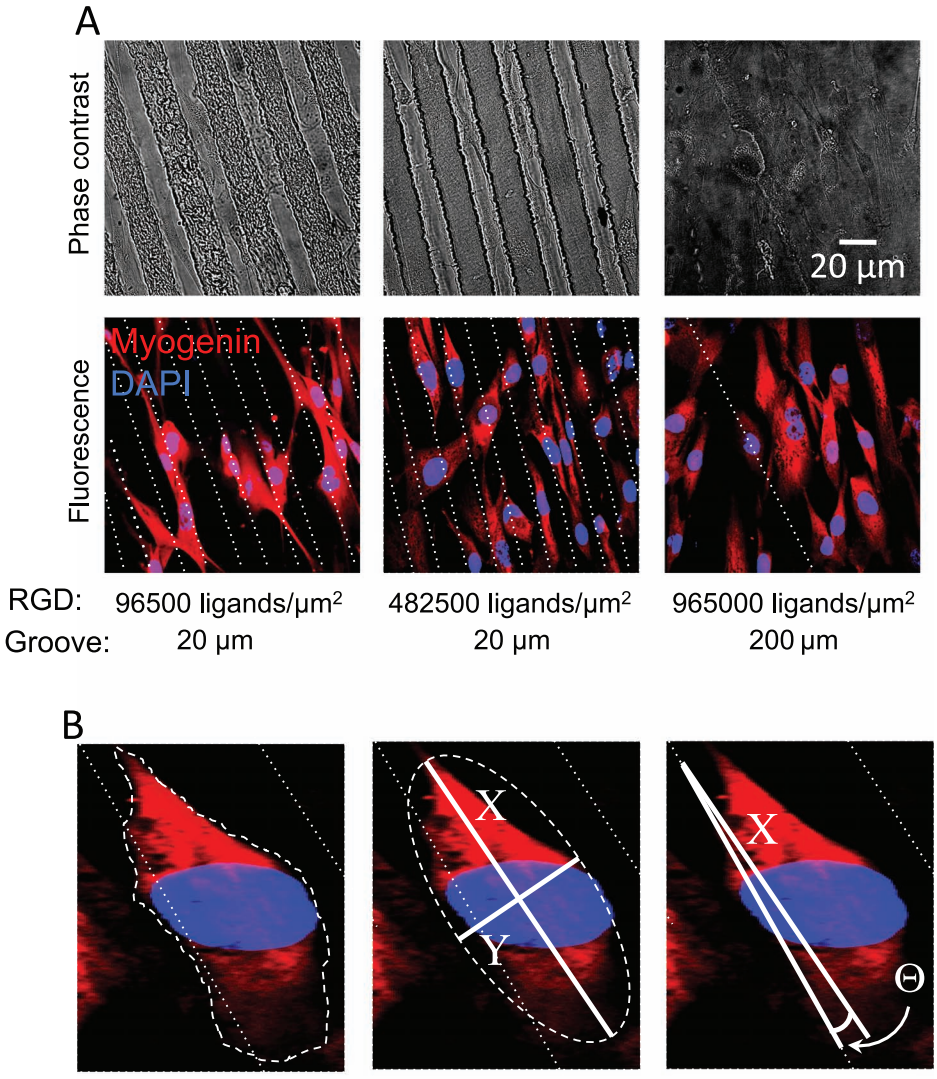

Figure 1. A) Representative micrographs of primary human myoblasts cultured on protein-engineered biomaterials. RGD density varies from 96500 to 965000 ligands/µm^2 and groove spacing varies from 20 to 200 µm. Micropattern topography is visualized by phase contrast microscopy (top) and as dashed white lines on fluorescent micrographs (bottom). Myoblasts are stained for myogenin (muscle cell marker, red) and counter-stained with DAPI (nuclear marker, blue). B) Representative quantification of cell morphology. Area within the perimeter is the total spread area (left). Each perimeter is computationally approximated by a best-fit ellipse with major (X) and minor (Y) axes to quantify the aspect ratio (X/Y, center). The angle between the cell major axis (X) and the micropattern determines cell alignment (right).

tested and stain positively for myogenin, a muscle cell marker (**Figure 1**, Figure S2 of the SI). Groove heights are designed to be ~5 µm; therefore, the side walls of the grooves do not physically restrict the cells (height ~10 µm), as clearly evident by myoblasts spreading across the boundaries between groove ridges and valleys (Figure 1). As a consequence, observed cell alignment is a result of topographical cues and not due to restriction of cell spreading. Qualitative analysis of cellular morphology suggests that myoblasts achieve greater alignment on smaller groove spacings (Figure 1A left and middle) and greater spreading on higher RGD densities (Figure 1A middle and right).

To further elucidate cellular responses, a rigorous quantitative analysis of single cell characteristics is performed. In particular, the cell alignment, spread surface area, and aspect ratio (i.e., elongation) are quantified for human myoblasts and C2C12 cells for each biomaterial condition (n > 900). To isolate the impact of groove spacing on myoblast morphology, we maintain a constant surface density of RGD cell-adhesion ligands at 965000 ligands/µm^2, which is the highest density possible for our system. Myoblast alignment is hypothesized to be an important promoter of fusion into myotubes.[19] Previous studies have reported that both C2C12 cells and mouse primary myoblasts exhibit greater alignment on substrates with smaller groove spacing.[1–4,7] Consistent with these results, we find that increasing the frequency of topographical cues (i.e., smaller groove spacing) promotes human primary myoblast alignment to the underlying substrate (quantified as depicted in Figure 1B, right panel). On wider groove spacings, human primary myoblasts exhibit an increased deviation

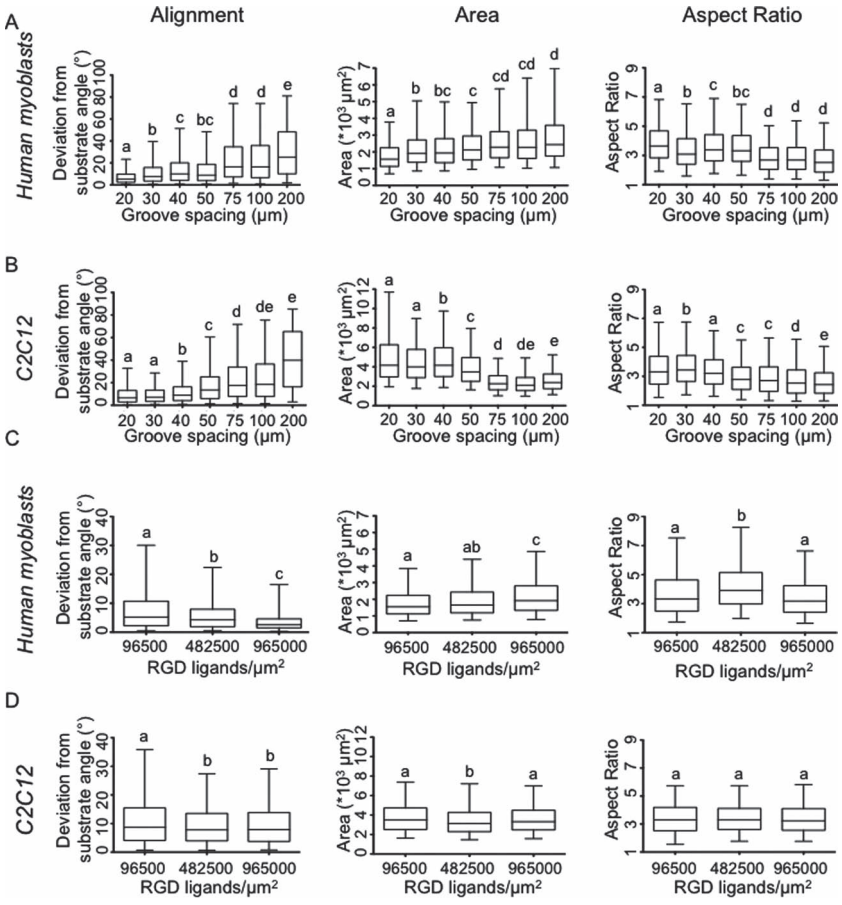

Figure 2. Human myoblast (A,C) and C2C12 cell (B,D) alignment, spread area, and aspect ratio in response to biomaterial microtopographical groove spacing (A,B) and cell-adhesive RGD ligand density (C,D). Data shown as box-and-whisker plots: box marks the 25th to 75th percentiles, horizontal line marks the median, whiskers mark the 5th to 95th percentiles. Letters over the bars represent statistical significance with a 99.9% confidence interval; bars with the same letters are statistically similar, while bars with different letters are statistically different.

from substrate angle (**Figure 2**A, left). As expected, the mouse-derived C2C12 cells exhibit the same response (Figure 2B, left). Cellular alignment requires cytoskeletal remodeling into an elongated morphology. The cell aspect ratio is defined as the ratio between the major and minor axes of the best-fit ellipse for the cell perimeter (Figure 1B, middle). As expected from our alignment data, we also find that human primary myoblast elongation increases with an increase in topographical cues (Figure 2A, right). Similarly, C2C12 elongation also increases with decreased groove spacing (Figure 2B, right), as expected from literature.[7] Therefore, with regard to alignment and elongation, C2C12 cells appear to be good predictors of human myoblast behavior.

While C2C12 cells can accurately predict primary human myoblast alignment and elongation behavior in response to topographical cues, discrepancies arise upon investigation of another parameter of cell morphology: cell spreading area. Wider groove spacings result in increased spreading of human myoblasts (Figure 2A, middle), but decreased spreading of C2C12 cells (Figure 2B, middle). It is also noteworthy that in general, C2C12 cells are more spread than human myoblasts; C2C12 cells exhibit spread areas up to 12000 µm^2, while the largest area for human primary myoblasts is 7000 µm^2. This highlights intrinsic differences between the immortalized, mouse-derived C2C12 cells and the primary myoblasts isolated from fresh human tissue. We hypothesized that human myoblast spread cell area, which is not well-modeled by the C2C12 line, may be a potent indicator of differentiation potential, because the larger the spread cell area is, the more cell-adhesive RGD ligands the cell is able to access. This ligand is recognized by multiple integrins including several containing the β1 integrin sub-unit,[20] which is required for myoblast fusion into myotubes.[21]

In order to further elucidate the impact of cell-adhesion ligand density on myoblast behavior, we systematically vary the density of the RGD ligand from 96500 to 965000 ligands/µm^2 (i.e., 16–160 pmol/cm^2) while keeping the groove spacing constant at 20 µm, thus providing the greatest number of topographical cues to the cells (Figure S1 and Supplemental Methods in the SI). RGD ligand density is specified by mixing the cell-adhesive, engineered protein with a second engineered protein that is otherwise identical except for the substitution of a scrambled amino acid sequence (RDG) that cannot be recognized by cell-surface integrin receptors.[15] Because the total protein weight percent and the amino acid content are kept constant across all biomaterials, the swelling ratio, hydrogel mesh size, and mechanical properties of the biomaterials remain unaffected, and the cell-adhesion ligand density is the only biomaterial parameter altered.[15] As RGD density increases, human myoblast cell area correspondingly increases (Figure 2C, middle), whereas C2C12 cell spreading is largely unaffected (Figure S2 of the SI), demonstrating that primary human myoblasts display greater sensitivity to RGD density than the model mouse cell-line. Similar results are obtained when cell alignment is assessed; human myoblasts exhibit significantly greater alignment on substrates with higher RGD density (Figure 2C, left), while C2C12 cells display only slight improvement (Figure 2D, left). Interestingly, while C2C12 cell aspect ratio is unresponsive to RGD density (Figure 2D, right), for human myoblasts, a bimodal distribution is observed, with maximum elongation at an intermediate RGD density (482500 ligands/µm^2). At higher RGD density (965000 ligands/µm^2), the increase in cell width is greater than the increase in cell length, resulting in a highly spread cell (Figure 2C, right). Previous work has demonstrated that C2C12 cells respond to changes in RGD density at lower concentrations (~1–10 fmol/cm^2 range),[5] suggesting that the number of ligands present in our fibronectin-elastin-like substrates may saturate all available C2C12 receptors even at the lowest densities tested (~16 pmol/cm^2).

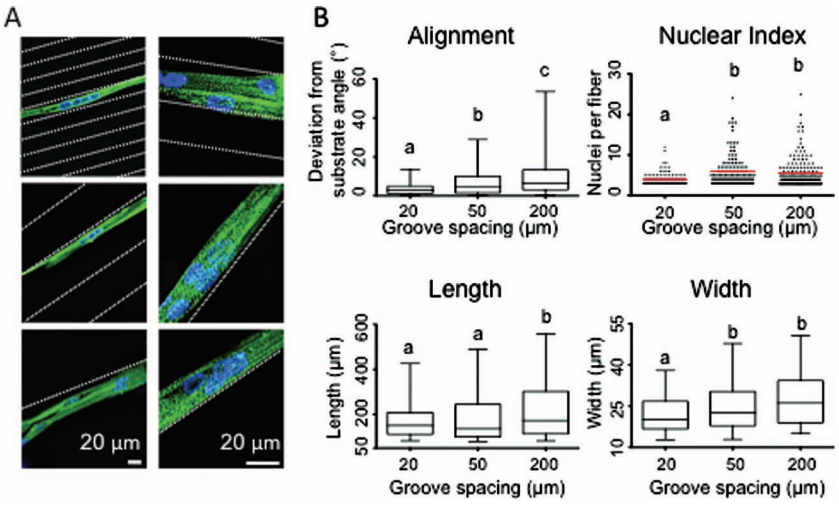

Figure 3. Human myotube differentiation on protein-engineered biomaterials. A) Fluorescent micrographs of myotubes stained for muscle myosin heavy chain (MMHC, green, left) or α-actinin, a marker of sarcomeric assembly (green, right) and counter-stained with DAPI nuclear marker (blue). B) Human myotube alignment, nuclear index, length, and width were measured as a function of microtopographical groove spacing. Box-and-whisker plots shown as in Figure 2; the nuclear index plot shows each individual myotube as a separate data point with the population median indicated by a red line.

Taken together, our results demonstrate that C2C12 cells are not accurate predictors of primary human myoblast responses to topographical cues or RGD ligand density. Therefore, human primary myoblasts were studied independently in further experiments to determine the role of engineered matrices in controlling *in vitro* myotube differentiation. Matrices with three representative groove spacings: small (20 μm), medium (50 μm), and large (200 μm), were fabricated with a cell-adhesion ligand density that initiated maximal myoblast spreading and alignment (965000 RGD ligands/μm^2). Differentiation of human myoblasts into extended, multinucleated myotubes ranging hundreds of microns in length is observed on all three matrix designs after 10 days of culture in differentiation medium (low-glucose, serum-free) (**Figure 3**A). Myotubes on matrices with higher frequencies of topographical cues exhibit greater alignment to the substrate (Figure 3B, top left). Interestingly, alignment with matrix topography is significantly increased at the myotube stage compared to the myoblast stage for all groove spacings. For example, even on the largest groove spacings (200 μm), myotube deviation from the substrate pattern has a median angle of only 7° (Figure 3B, top left), while myoblast deviation is greater than 25° (Figure 2A, left). This striking difference underscores the need to quantify cellular morphology during both the myoblast and myotube stages. Furthermore, these data suggest that the differentiation process itself facilitates myotube alignment to underlying topographical cues.

Matrix topography is also found to have a significant effect on myotube dimensions. In general, as groove spacing increases, myotube length and width also increases, although a large population heterogeneity is observed (Figure 3). Myotube widths range from 12–50 μm, while myotube lengths between 75–550 μm are observed. Consistent with previous C2C12 studies,[1] we find that wider groove spacings cause an increase in nuclear index (i.e., number of nuclei per myotube), which is considered a marker of myotube maturity.[1] A median of 4 nuclei per myotube is observed on 20 μm-grooved substrates, while a median of 6 nuclei per myotube is present on wider grooves. Similarly, the percentage of more highly nucleated myotubes (>10 nuclei) is 2%, 13%, and 11% on substrates with 20, 50, and 200 μm-spaced grooves, respectively. These data demonstrate that myotube morphology can be directly altered by controlling biomaterial topography.

From these results, it appears that myoblast cell area, which is the highest on the 200 μm grooves, is the most potent predictor of differentiation potential. Substrates with the fewest topographical cues result in both the highest degree of cell spreading and the longest and widest multinucleated myotubes. In contrast, increases in myoblast elongation and alignment, which occurred on smaller groove spacings, do not correlate with extended myotube formation. Towards the larger goal of creating an *ex vivo* mimic of human skeletal tissue, we also test for markers of myotube maturity that are required to recapitulate *in vivo* functionality such as contractility. We first stain for α-actinin, which is a marker of sarcomeric assembly. Sarcomeres are organized in a repeating fashion within contractile muscle fibers and consist of force-generating proteins. Sarcomere organization is evident in myotubes differentiated on all three matrix designs (Figure 3A, right panel). To demonstrate functional activity of the sarcomeres, myotubes are paced using external electrodes (10 volts, 1 Hz), resulting in isolated myotube contractions (Video S1 of the SI). To the best of our knowledge, this is the first published report of externally paced human contractile myotubes cultured *ex vivo*.

In conclusion, we have successfully differentiated primary myoblasts isolated from human biopsies into contractile myotubes on a novel biomaterial. The spread area of individual myoblasts was identified as a predictor of myotube differentiation, and we demonstrated control over human myotube architecture (i.e., length, width, and nuclear index) through engineering of biomaterial substrate cues. Importantly, we observed that myoblast-matrix interactions were not effectively modeled by immortalized, mouse-derived C2C12 cells. This *in vitro* human skeletal muscle tissue model will be useful in studies of human myotube differentiation, maturation, and function. For example, a recent study showed that smooth muscle cells (a different muscle type found in vascular tissue that is capable of contracting as single cells) demonstrated increased contractility in response to increased elongation.[22] Our engineered cell-biomaterial system is well suited for future studies looking at the impact of biomaterial cues on contractility and force generation in the context of skeletal muscle. Further, these results suggest the potential *ex vivo* development of muscle fibers tailored for specific tissue engineering applications. Because the utilized biomaterial is biodegradable and biocompatible this work provides the foundation for future regenerative medicine applications aimed at replacing aged, injured, or diseased skeletal muscle tissue.

Experimental Section

Protein crosslinking: Engineered protein (0.1 mg/μL in phosphate-buffered saline (PBS) at 4 °C) was crosslinked with tetrakis(hydroxymethyl)-phosphonium chloride (THPC) between a soft lithographic mold and aminated glass as further detailed in Supplemental Information.

Cell culture: Primary human myoblasts were derived from skeletal muscle biopsies isolated at Stanford University Hospital from patients during routine surgeries according to previously described methods.[23] C2C12 cells were cultured following supplier protocols. Cells were seeded at 500 cells/mm^2 onto biomaterials and analyzed at 24 h for myoblast experiments and at 10 d for myotube experiments. A myotube was defined as any multinucleated structure containing 3 or more nuclei (which distinguishes myoblast cell division from myoblast fusion). Myotubes were electrically paced with an IonOptix Myopacer Cell Stimulator (10 V, 1 Hz).

Cell quantification and statistical analysis: ImageJ analysis of immunostained confocal micrographs were used to quantify cell morphology ($n > 900$ cells per condition for myoblast stage, $n > 100$ for myotubes). Statistical significance was determined using the Kruskal–Wallis test with 99.9% confidence interval.

Supporting Information

Supporting Information is available from the Wiley Online Libray or from the author.

Acknowledgements

The authors acknowledge funding from NIH K99-AR061465 to P.M.G.; NIH DP2-OD006477, NIH R21-AR062359, and NSF DMR-0846363 to S.C.H.; NIH HL096113, NIH HL100397, NIH AG020961, NIH AG009521, JDRF 34-2008-623, MDA 4320, CIRM RT1-01001, LLS TRP 6025-09, Fulbright Specialist Grant from CIES, Mayent/Rothschild Fellowship and the Baxter Foundation to H.M.B. We thank Dr. Stephane Corbel for isolation of human myoblast cells.

Received: June 10, 2012
Published online: September 5, 2012

[1] P. Bajaj, B. Reddy Jr., L. Millet, C. Wei, P. Zorlutuna, G. Bao, R. Bashir, *Integr. Biol.* **2011**, *3*, 897.
[2] J. L. Charest, A. J. Garcia, W. P. King, *Biomaterials* **2007**, *28*, 2202.
[3] M. T. Lam, Y.-C. Huang, R. K. Birla, S. Takayama, *Biomaterials* **2009**, *30*, 1150.
[4] M. T. Lam, S. Sim, X. Zhu, S. Takayama, *Biomaterials* **2006**, *27*, 4340.
[5] J. A. Rowley, D. J. Mooney, *J. Biomed. Mater. Res. A* **2002**, *60*, 217.
[6] N. F. Huang, S. Patel, R. G. Thakar, J. Wu, B. S. Hsiao, B. Chu, R. J. Lee, S. Li, *Nano Lett.* **2006**, *6*, 537.
[7] P.-Y. Wang, H.-T. Yu, W.-B. Tsai, *Biotechnol. Bioeng.* **2010**, *106*, 285.
[8] A. J. Engler, M. A. Griffin, S. Sen, C. G. Bonnemann, H. L. Sweeney, D. E. Discher, *J. Cell Biol.* **2004**, *166*, 877.
[9] R. Shah, A. C. M. Sinanan, J. C. Knowles, N. P. Hunt, M. P. Lewis, *Biomaterials* **2005**, *26*, 1497.
[10] S. A. Riboldi, M. Sampaolesi, P. Neuenschwander, G. Cossu, S. Mantero, *Biomaterials* **2005**, *26*, 4606.
[11] C. A. Powell, B. L. Smiley, J. Mills, H. H. Vandenburgh, *Am. J. Physiol.: Cell Physiol.* **2002**, *283*, C1557.
[12] L. Boldrin, A. Malerba, L. Vitiello, E. Cimetta, M. Piccoli, C. Messina, P. G. Gamba, N. Elvassore, P. De Coppi, *Cell Transplantation* **2008**, *17*, 577.
[13] M. A. Brady, M. P. Lewis, V. Mudera, *J. Tissue Eng. Regener. Med.* **2008**, *2*, 408.
[14] E. Serena, S. Zatti, E. Reghelin, A. Pasut, E. Cimetta, N. Elvassore, *Integr. Biol.* **2010**, *2*, 193.
[15] K. S. Straley, S. C. Heilshorn, *Soft Matter* **2009**, *5*, 114.
[16] D. Sengupta, S. C. Heilshorn, *Tissue Eng., Part B* **2010**, *16*, 285.
[17] N. H. Romano, D. Sengupta, C. Chung, S. C. Heilshorn, *Biochim. Biophys. Acta* **2011**, *1810*, 339.
[18] J. R. Sanes, *J. Cell Biol.* **1982**, *93*, 442.
[19] M. J. O. Wakelam, *Biochem. J.* **1985**, *228*, 1.
[20] J. D. Humphries, A. Byron, M. J. Humphries, *J. Cell Sci.* **2006**, *119*, 3901.
[21] M. Schwander, M. Leu, M. Stumm, O. M. Dorchies, U. T. Ruegg, J. Schittny, U. Muller, *Dev. Cell* **2003**, *4*, 673.
[22] P. W. Alford, A. P. Nesmith, J. N. Seywerd, A. Grosberg, K. K. Parker, *Integr. Biol.* **2011**, *3*, 1063.
[23] H. M. Blau, C. Webster, *Proc. natl. Acad. Sci. USA* **1981**, *78*, 5623.